Mon. Not. R. Astron. Soc. **000**, 000–000 (0000) Printed 4 February 2008 (MN LATEX style file v2.2)

Photometric studies of three multiperiodic β Cephei stars: β CMa, 15 CMa and KZ Mus

R. R. Shobbrook,[1] G. Handler,[2] D. Lorenz,[2] D. Mogorosi [3]

[1] *Research School of Astronomy and Astrophysics, Australian National University, Canberra, ACT, Australia*
[2] *Institut für Astronomie, Universität Wien, Türkenschanzstrasse 17, A-1180 Wien, Austria*
[3] *Department of Physics, University of the North-West, Private Bag X2046, Mmabatho 2735, South Africa*

arXiv:astro-ph/0603754v1 28 Mar 2006

Accepted 2005 July 17. Received 2005 August 13; in original form 2005 September 10

ABSTRACT

We have carried out single and multi-site photometry of the three β Cephei stars β and 15 CMa as well as KZ Mus. For the two stars in CMa, we obtained 270 h of measurement in the Strömgren uvy and Johnson V filters, while 150 h of time-resolved Strömgren uvy photometry was acquired for KZ Mus. All three stars are multi-periodic variables, with three (β CMa) and four (15 CMa, KZ Mus) independent pulsation modes. Two of the mode frequencies of 15 CMa are new discoveries and one of the known modes showed amplitude variations over the last 33 years. Taken together, this explains the star's diverse behaviour reported in the literature fully.

Mode identification by means of the amplitude ratios in the different passbands suggests one radial mode for each star. In addition, β CMa has a dominant $\ell = 2$ mode while its third mode is nonradial with unknown ℓ. The nonradial modes of 15 CMa, which are $\ell \leqslant 3$, form an almost equally split triplet that, if physical, would imply that we see the star under an inclination angle larger than 55°. The strongest nonradial mode of KZ Mus is $\ell = 2$, followed by the radial mode and a dipole mode. Its weakest known mode is nonradial with unknown ℓ, confirming previous mode identifications for the star's pulsations.

The phased light curve for the strongest mode of 15 CMa has a descending branch steeper than the rising branch. A stillstand phenomenon during the rise to maximum light is indicated. Given the low photometric amplitude of this nonradial mode this is at first sight surprising, but it can be explained by the mode's aspect angle.

Key words: stars: variables: other – stars: early-type – stars: oscillations – stars: individual: β CMa – stars: individual: 15 CMa – stars: individual: KZ Mus – techniques: photometric

1 INTRODUCTION

The β Cephei stars are a group of early B-type stars with masses between 9 and 17 $M_\odot$ that exhibit light, radial velocity and line-profile variability on time scales between 2–8 hours (Stankov & Handler 2005). The cause of their variability is pulsation in pressure and gravity modes of low radial order. About 110 definite members of this group are known in our Galaxy (Stankov & Handler 2005, Pigulski 2005, Handler 2005), but a large number of candidates was also revealed in the Large Magellanic Cloud (Kołaczkowski et al. 2004).

One of the major astrophysical applications of the β Cephei stars is asteroseismology, the determination of the interior structure of pulsating stars via theoretical modelling of their normal mode spectra. All main-sequence pulsators more massive than the Sun that have been studied asteroseismically so far, and where unambiguous results on stellar structure could be obtained (e.g. see Pamyatnykh, Handler & Dziembowski 2004), belong to the β Cephei stars.

The main prerequisite for an asteroseismic study is that a number of pulsation modes large enough is known to remove any ambiguities concerning the position of the star in the HR diagram, and that these modes are unambiguously identified with their pulsational quantum numbers, k, the radial overtone of the mode, the spherical degree ℓ, and the azimuthal order m. Even among the β Cephei stars, such objects are not easy to find, which can often be traced to

insufficient data that are incapable of providing the required mode frequency resolution and number of mode detections.

Consequently, it is worthwhile to select potentially promising targets and to obtain reasonably large amounts of time-resolved photometric and/or spectroscopic data so that a reliable assessment of their asteroseismic promise can be made. For the present work, we have chosen three stars that seemed to justify such an effort.

The conspicuous naked-eye star ($V = 1.98$) β CMa is known as a radial-velocity variable for more than a hundred years (see Struve 1950). Shobbrook (1973a) obtained the first extensive photometric data set for this star and analysed it together with the radial velocities previously published. He found three pulsation periods for the star, and suggested that all of them changed somewhat over the years. As his measurements were taken in the V filter only, no photometric mode identification could be made, but the different light-to-radial-velocity amplitudes of the two strongest modes noticed by Shobbrook (1973a) suggest that they have different ℓ. However, we should note that this conclusion is based on the assumption that both modes had the same intrinsic amplitude at the different epochs of the photometric and spectroscopic measurements.

15 CMa ($V = 4.80$) shows notoriously difficult variability according to the literature. This began with the first claim of its radial velocity variability (Campbell 1911) that was later retracted (Moore 1936). Among the successive studies of its variability, the photometric investigation by Shobbrook (1973b) was the most extensive. He identified the period of the dominant variation in his light curves, and noted its non-sinusoidal shape, but could not push the analysis further. Heynderickx (1992) suggested the presence of at least two pulsation modes, which were later identified with $\ell = 2$ and 0, respectively, on the basis of multicolour photometry (Heynderickx, Waelkens & Smeyers 1994).

KZ Mus ($V = 9.1$) has been studied during a two-site photometric effort by Handler et al. (2003). These authors also review the (short) history of the investigations of its variability. They found four independent modes in the stellar light variations, where the strongest of these have $\ell = 2$, 0 and 1, respectively, and the radial mode is either the fundamental or the first overtone. The presence of additional pulsation modes was suspected by Handler et al. (2003), who also pointed out the importance of an identification of the spherical degree of the fourth known mode.

2 OBSERVATIONS AND REDUCTIONS

We acquired time-resolved differential photoelectric photometry of all the three targets. The bright stars β and 15 CMa were measured with respect to the comparison stars HR 2271 ($V = 5.8$, B3II/III) and 17 CMa ($V = 5.8$, A2V), that were observed alternating with the targets. No evidence for variability of the latter two stars within a limit of 1.5 mmag was found.

This group of four stars was observed from three observatories in the time span of November 2004 to February 2005. Thirty-five nights of Strömgren *uvy* data were obtained at Siding Spring Observatory, Australia, with the 0.6-m telescope. Eighteen nights were acquired with the 0.5-m telescope at the South African Astronomical Observatory. The Johnson V filter was used for the first five nights; the remaining 13 nights consist of Strömgren *uvy* data, but the u filter was not used for β CMa at this site. Finally, ten nights of measurement were performed with the 0.75-m Automated Photometric Telescope T6 at Fairborn Observatory, USA, again using Strömgren *uvy* filters. Neutral density filters were used in all cases to avoid photomultiplier destruction, owing to the extreme brightness of β CMa; the same neutral density filters were applied to all stars at each site. The total of 63 nights of observation has a time base of 111.95 d, corresponding to 272.7 h of measurements of β CMa and 265.4 h of measurements for 15 CMa, respectively.

KZ Mus was measured with the same observational technique. The comparison stars were HD 110022 ($V = 7.8$, B8 III/IV), which was replaced by HD 109082 ($V = 8.1$, B9IV) after the first few nights when we found evidence for variability of the former object. The second comparison star was HD 111876 ($V = 7.1$, B9.5/A0V). HD 109082 was constant during the observations. However, HD 111876 showed a small (~ 0.01 mag in all three filters) mean magnitude drift during the total time span of observations.

This group of stars was observed from March to June 2005, but with the 0.6-m telescope at Siding Spring Observatory only. Data were acquired during 27 nights, giving a total time span of 98.9 d, and 154.3 h of measurement resulted. Again the Strömgren *uvy* filters were used, but no neutral density filters had to be employed.

Data reduction comprised a correction for coincidence losses, subtraction of sky background and extinction determination and correction. Whenever possible, nightly extinction coefficients were determined with the classical Bouguer method (fitting a straight line to a plot of magnitude vs. air mass) from the measurements of the two comparison stars. For the remaining nights, mean coefficients from the adjoining nights were used.

The magnitudes of the comparison stars were adjusted to their mean differences, and were then combined into a curve that was assumed to reflect the effects of sky transparency and detector sensitivity changes only. Subsequently, these combined time series were binned into intervals that would allow good compensation for the above-mentioned non-intrinsic variations in the target star time series and were subtracted from the measurements of the variables. The binning minimises the introduction of noise in the differential light curves of the targets.

The timings for the differential light curves were heliocentrically corrected as the next step. Finally, the photometric zeropoints of the different instruments were compared between the different sites and were adjusted if necessary. Measurements in the Strömgren y and Johnson V filters were treated as equivalent due to the similar effective wavelengths of these filters, and were analysed jointly after a correction for differential colour extinction in V. Some example light curves of our three targets together with multifrequency solutions to be discussed in the following are shown in Figs. 1, 2 and 3, respectively.

3 FREQUENCY ANALYSIS

Our frequency analysis was mainly performed with the program `Period98` (Sperl 1998). This package applies single-

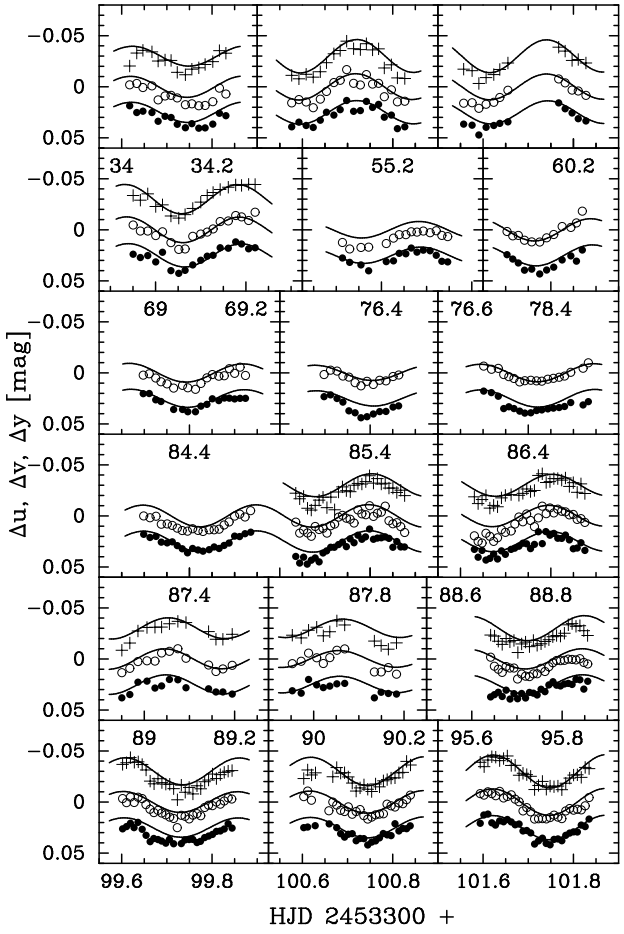

Figure 1. Some of our observed light curves of β CMa. Plus signs are data in the Strömgren u filter, opem circles are our v measurements and filled circles represent Strömgren y data. The full line is a fit composed of all the periodicities detected in the light curves (Table 2). The amount of data displayed is approximately one third of the total.

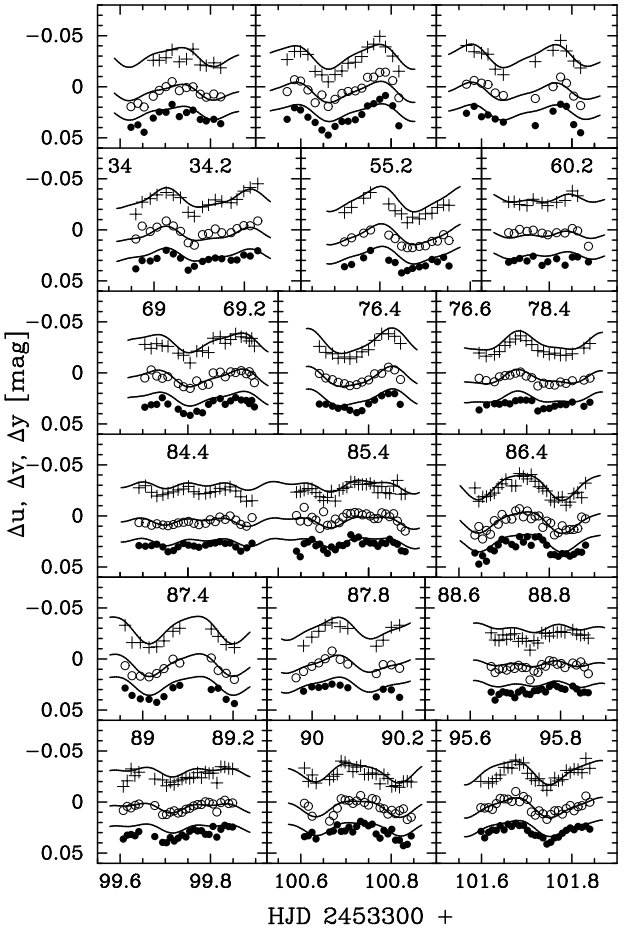

Figure 2. Some of our observed light curves of 15 CMa. Plus signs are data in the Strömgren u filter, open circles are our v measurements and filled circles represent Strömgren y data. The full line is a fit composed of all the periodicities detected in the light curves (Table 3). The amount of data displayed is approximately one third of the total.

frequency power spectrum analysis and simultaneous multi-frequency sine-wave fitting. It also includes advanced options such as the calculation of optimal light-curve fits for multi-periodic signals including harmonic, combination, and equally spaced frequencies. Our analysis will require some of these features.

3.1 β CMa

We started by computing the Fourier spectral window of the u filter data. It was calculated as the Fourier transform of a single noise-free sinusoid with a frequency of 3.979 cd^{-1} (the strongest pulsational signal of β CMa) and an amplitude of 12 mmag, sampled in the same way as our measurements. The upper panel of Fig. 4 contains the result. The alias structures in this window are sufficiently suppressed to allow easy and unique determinations of the frequencies of the stellar light variations.

We proceeded to compute the amplitude spectra of the data themselves (second panel of Fig. 4). The signal designated f_1 dominates. We prewhitened it by subtracting a synthetic sinusoidal light curve with a frequency, amplitude and phase that yielded the smallest possible residual variance. We then computed the amplitude spectrum of the residual light curve, which is shown in the third panel of Fig. 4.

A second signal (f_2) can clearly be seen in this graph. Prewhitening it leaves no further significant periodicities in the u data alone. At this stage, we prewhitened the data from the v and y filters by the f_1 and f_2 frequencies, then combined these residuals with those from the u filter data divided by 1.2. This 1.2 factor scales the u data to the same amplitude as that found for f_1 in the v and y data. This procedure is valid because the light curves of β Cephei stars have the same phase at all optical wavelengths.

The residual amplitude spectrum of the uvy data combined in this way is shown in the lowest panel of Fig. 4. We note the presence of another signal, f_3, and include it in our frequency solution for β CMa. Prewhitening by this variation as well, we find no further significant periodicity in our combined residual amplitude spectrum.

We consider an independent peak statistically significant if it exceeds an amplitude signal-to-noise ratio of 4 in the periodogram; combination signals must satisfy $S/N >$ 3.5 to be regarded as significant (see Breger et al. 1993,

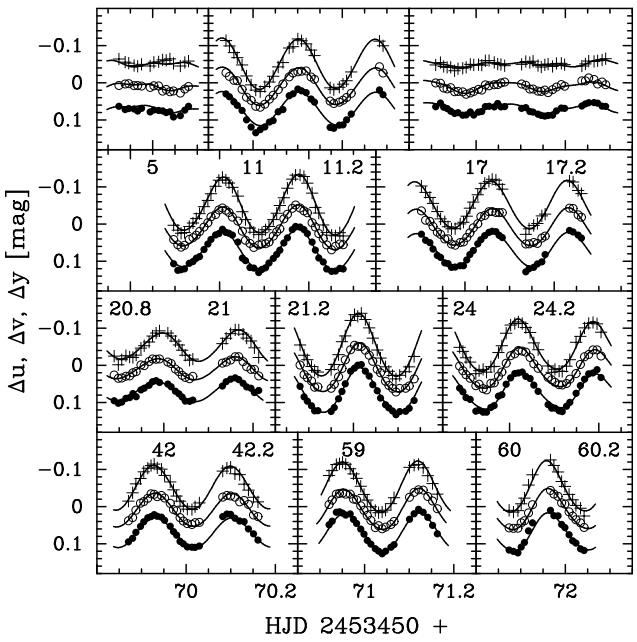

Figure 3. Some of our observed light curves of KZ Mus. Plus signs are data in the Strömgren u filter, opem circles are our v measurements and filled circles represent Strömgren y data. The full line is a fit composed of all the periodicities detected in the light curves (Table 4). The amount of data displayed is approximately half the total.

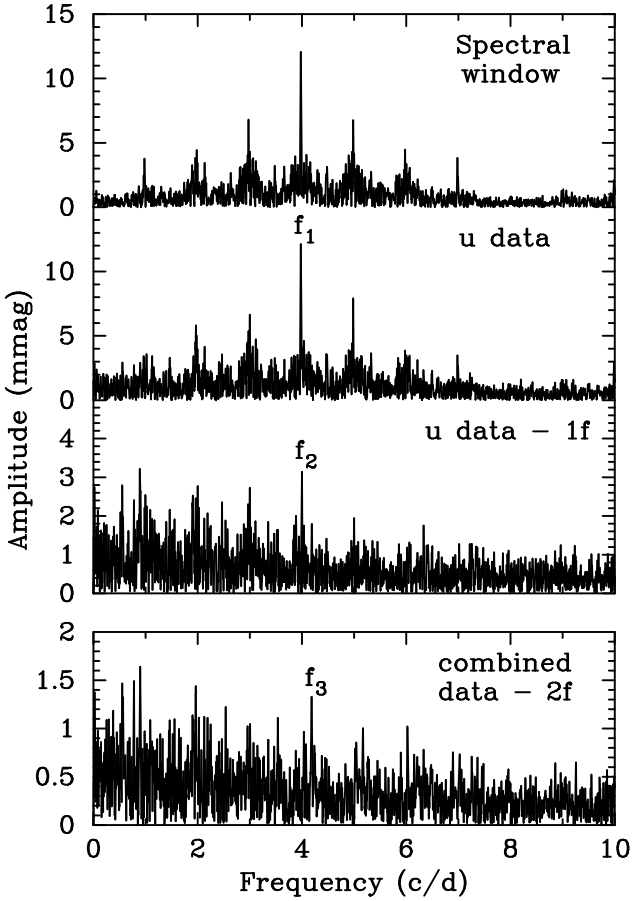

Figure 4. Amplitude spectra of β CMa. The uppermost panel shows the spectral window of the data, followed by the periodogram of the data. Successive prewhitening steps are shown in the following panels; note their different ordinate scales.

1999 for a more in-depth discussion of this criterion). The noise level was calculated as the average amplitude in a 5 cd^{-1} interval centred on the frequency of interest.

We are now in a position to determine a final multifrequency solution for our light curves of β CMa. To this end, we first computed a weighted average for the frequencies derived from the individual filters' data, where the weight corresponded to the S/N of the signals. The results were adopted as our final frequency values. We then fitted these frequencies to the *uvy* data and determined their amplitudes and phases (that were, as assumed previously, found to be the same for all filters within the errors). The final solution is listed in the upper part of Table 1.

The error estimates we give are the formal values for the amplitudes (Montgomery & O'Donoghue 1999). We note that such formal error bars are expected to underestimate the real errors by about a factor of 2 (Handler et al. 2000, Jerzykiewicz et al. 2005). For the frequencies themselves, we computed both the formal errors, and the deviation of the mean of the values from the individual filters; we then adopted the larger of the two values. For frequencies f_1 and f_3 the two results agreed quite well (within 10 per cent). However, the error of the mean was a factor of 2 larger for f_2.

This result can be easily understood: within the time span of our data, f_2 is not fully resolved from a possible variation of 4 cycles per sidereal day. Such a variation could be present in our light curves due to residual (colour) extinction effects, despite our careful data reduction. This interpretation is supported by the observation that the value of f_2 is closest to 4 cycles per sidereal day in the u band where possible residual extinction effects are expected to be

Table 1. Multifrequency solutions for photometric data of β CMa. Error estimates (following Montgomery & O'Donoghue 1999) on the amplitudes are ± 0.4 mmag in u and ± 0.3 mmag in v and y, respectively. The S/N ratio was computed following Breger et al. (1993) and is quoted for the v filter.

ID	Freq. (cd^{-1})	u Amp. (mmag)	v Amp. (mmag)	y Amp. (mmag)	S/N
New photometry					
f_1	3.9793 ± 0.0001	12.0	10.6	10.0	25.5
f_2	3.9994 ± 0.0007	3.8	1.7	1.3	4.1
f_3	4.1857 ± 0.0007	1.7	1.7	1.4	4.2
Archival data					
f_1	3.9792 ± 0.0001			10.3 (V)	28.5
f_2	3.9999 ± 0.0007			1.9 (V)	5.2
f_3	4.1821 ± 0.0009			1.4 (V)	4.0

largest. We must therefore be careful in the interpretation of the frequency and *uvy* amplitudes of f_2.

3.1.1 Reanalysis of archival data

One of us (RRS) has digitised his archival V filter photometry of β and 15 CMa taken in the early 1970s. We can therefore analyse these measurements with our frequency analysis methods, allowing a direct comparison of the results.

For β CMa we confirm the findings by Shobbrook (1973a, see lower part of Table 1): we obtain the same three frequencies as he did. Given the probable underestimation of the real errors of the frequencies and amplitudes (especially for mode f_2), we are reluctant to claim the presence of amplitude and/or frequency variability for the star.

On the other hand, we note that there seems to be some low-frequency variability, for which we are unable to determine a period, remaining in the residuals, similar to what can be discerned in the lowest panel of Fig. 4. We find this behaviour in all independent data sets we have for β CMa, but not in the differential light curve of the two comparison stars. Because we can exclude an extinction effect for its origin, we are inclined to believe that this variation is intrinsic to our target star.

We attempted to obtain an improved frequency solution and to check for amplitude and frequency variability of the stellar pulsation modes by analysing the combined visual photometric data by Shobbrook (1973a), Balona et al. (1996) and the HIPPARCOS satellite (ESA 1997) together with our measurements. Regrettably, the amount and temporal separation of the data render this investigation inconclusive: we derive a best-fitting frequency for the strongest mode of $3.9793334 \pm 0.0000009\,\mathrm{cd}^{-1}$ that is slightly variable in amplitude and phase, but we cannot be certain whether this is a numerical artifact due to beating with the close mode at $3.9994\,\mathrm{cd}^{-1}$ when unresolved in certain subsets of data.

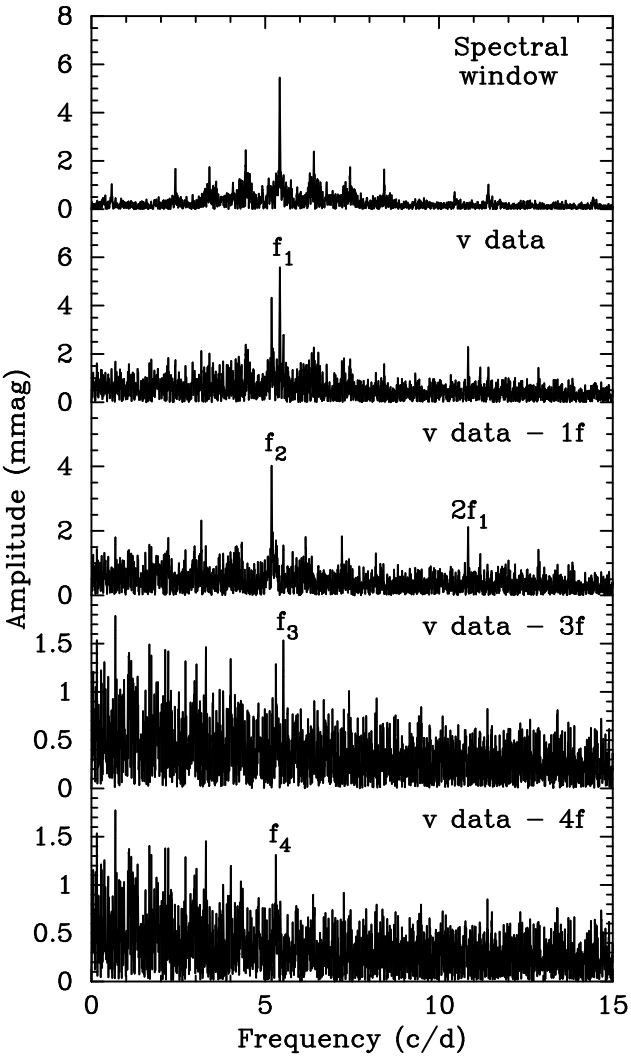

Figure 5. Amplitude spectra of 15 CMa. The uppermost panel shows the spectral window of the data, followed by the periodogram of the data. Successive prewhitening steps are shown in the following panels; note their different ordinate scales.

3.2 15 CMa

The frequency analysis for this star was carried out in a similar way as that for β CMa and is illustrated in Fig. 5. This time we use the v data for display as they resulted in the light curves of best S/N. In the case of 15 CMa, the spectral window had a single noise-free sinusoid with a frequency of $5.419\ \mathrm{cd}^{-1}$ and an amplitude of 5.4 mmag as input (upper panel of Fig. 5). The amplitude spectrum of the data themselves (second panel) already makes it clear that more than one frequency is present in the light curves. Prewhitening the strongest signal (f_1) leaves two conspicuous peaks in the residual amplitude spectrum. One of these is the first harmonic of f_1. Further prewhitening with these three signals indicates the presence of another periodicity, and prewhitening that one as well reveals a fourth independent frequency in the light curves. Pushing the analysis further, also by combining the residuals for the u, v and y data, as we did for β CMa, did not result in the detection of additional periodicities.

The final multifrequency solution for 15 CMa was determined in the same way as for β CMa: by computing S/N-weighted averages of the frequencies determined from the individual filters' data. We note that, for reasons of better accuracy, we fixed the frequency of the harmonic signal to exactly twice the value of the parent mode with `Period 98`.

We then recomputed the *uvy* amplitudes with these "best" frequencies and list the result in Table 2. Again, the adopted error estimates on the frequencies correspond to the larger of the two values derived from analytic formulae and rms deviations of the mean of the frequencies.

3.2.1 Reanalysis of archival data

We analysed the V measurements of 15 CMa by Shobbrook (1973b, also digitised by RRS), who also detected our signal f_1 and its first harmonic. However, he could not continue to search for further frequencies because the residual amplitude spectrum was too complicated.

Thanks to our multi-site measurements, we know four pulsation frequencies of the star without aliasing ambiguities, and we can use this information in our reanalysis. This helps us to solve the puzzle that the data by Shobbrook

Table 2. Multifrequency solution for time-resolved photometric data of 15 CMa. Error estimates (following Montgomery & O'Donoghue 1999) on the amplitudes are ± 0.3 mmag in u and ± 0.2 mmag in v and y, respectively. The S/N ratio was computed following Breger et al. (1993, 1999) and is quoted for the v data.

ID	Freq. (cd^{-1})	u Amp. (mmag)	v Amp. (mmag)	y Amp. (mmag)	S/N
New photometry					
f_1	5.4187 ± 0.0002	6.2	5.4	4.6	16.0
f_2	5.1831 ± 0.0003	5.4	3.9	2.9	11.2
$2f_1$	10.8374	2.4	2.1	2.1	7.2
f_3	5.5212 ± 0.0008	2.0	1.6	1.3	4.7
f_4	5.3085 ± 0.0012	1.6	1.4	1.1	4.2
Archival data					
f_1	5.4180 ± 0.0003			4.8 (V)	12.3
$2f_1$	10.8359			1.9 (V)	6.2
f_2	5.1845 ± 0.0009			1.5 (V)	3.8
f_3	5.5253 ± 0.0007			1.9 (V)	4.9
f_4	5.3103 ± 0.0008			1.6 (V)	4.3

(1973b) provided: we first detect f_1 and its harmonic. The three other frequencies detected in our new measurements are also present in the older photometry, and all three are required to explain the observations, as proven by different prewhitening trials. We list the result of this analysis in the lower part of Table 2. We point out that f_2 has a S/N below 4, but since it is known to be an intrinsic signal from our new measurements, we only require $S/N > 3.5$ to accept this frequency as real in the old data.

In this case, f_2 can be safely claimed as having varied in amplitude, whereas no such statement can be made for the other signals. In this context it is interesting to revisit the discussion of the Geneva data by Heynderickx (1992), who also observed 15 CMa. He detected our f_1 and its harmonic, but then encountered two closely spaced signals around f_2, where the frequency difference of these signals is close to the inverse time span of his data set. Consequently, it can be suspected that these two apparent signals near f_2 could in fact be due to a single mode with amplitude variability during Heynderickx' observations. We note that an attempt to refine the pulsation frequencies of the star by analysing the measurements by Shobbrook (1973b) and the HIPPARCOS satellite (ESA 1997) together with ours did not bear fruit due to aliasing problems.

We also note that, just as for β CMa, some slow aperiodic variability seems to be left in the residuals of both the archival and the new measurements. This slow variability is not correlated with the one of β CMa (neither in the old nor in the new data), which is further support for the idea that it is intrinsic to the stars and is not an instrumental effect.

3.2.2 The light curve shape of f_1

The amplitude of the harmonic frequency of f_1 is unusually high given the amplitude of the independent mode to which it is connected. We have therefore examined the shape of the light curve due to this mode. We fitted the five known frequencies of 15 CMa to the archival data and to our new measurements and then prewhitened the fit composed of the resulting parameters for f_2, f_3 and f_4. We then phased the residuals with f_1 and show the results in Fig. 6.

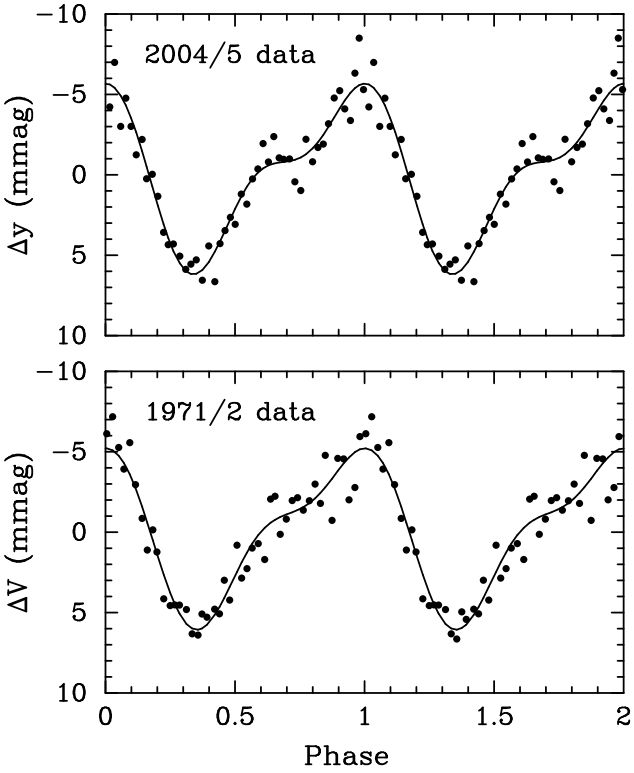

Figure 6. Phase diagram of light curves of 15 CMa with respect to f_1 (full dots), compared to a fit computed with f_1 and $2f_1$. Two cycles of the variation are shown. The rising branch of this light variation is flatter as the descending branch, and there seems evidence for a stillstand before light maximum.

The phase diagrams obtained in this way appear odd for a pulsating star: the rising branch of the light curve is less steep than the descending branch. When computing a fit to these phase diagrams composed of f_1 and $2f_1$, or when averaging the two phase diagrams, it even seems possible that there is a "stillstand" phenomenon in the rising branch. We would however like to see more data on the star before coming to a definite conclusion on this matter.

It is interesting to note that the scatter in the two phase diagrams are very similar: although smaller in number, the precision of the measurements taken in the 1970s is slightly better than that of our present data.

3.3 KZ Mus

The frequency analysis for this star was carried out in a similar fashion as for the others. We determined individual frequencies step-by-step and found four independent modes (see Fig. 7) plus three combination frequencies. Again, the frequencies were first determined for each individual filter, using `Period 98` to fix the frequencies of combination signals to the exact sums predicted by those of parent modes. Then, S/N-weighted averages of the frequencies determined from the individual filters' data were computed and adopted

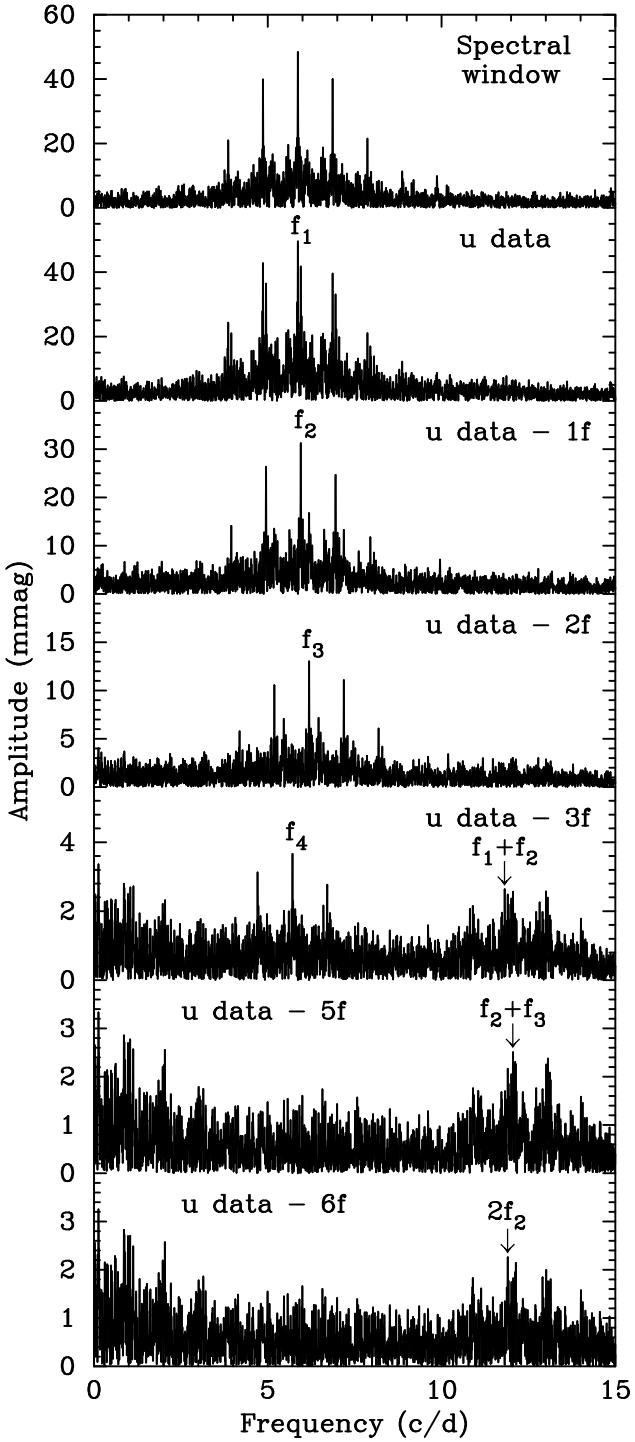

Figure 7. Amplitude spectra of KZ Mus. The uppermost panel shows the spectral window of the data, followed by the periodogram of the data. Successive prewhitening steps are shown in the following panels; note their different ordinate scales.

as our final frequency values. Our multifrequency solution obtained this way is listed in Table 3.

Comparing our results to those by Handler et al. (2003), we cannot find significant evidence for amplitude or frequency variability, but we do note the occurrence of a new combination frequency, $f_1 + f_3$. This signal is actually present in the older measurements, but we were not convinced about its reality during the previous analysis.

On the other hand, the combination signal $f_2 - f_1$ detected by Handler et al. (2003) is not present in our new measurements. This is likely due to the increased low-frequency noise in the new data caused by the variability of the comparison star HD 111876, which we were not able to remove satisfactorily.

Table 3. Multifrequency solution for our new time-resolved photometry of KZ Mus. Error estimates (following Montgomery & O'Donoghue 1999) on the amplitudes are ± 0.4 mmag in u and v, and ± 0.3 mmag in y. The S/N ratio was computed following Breger et al. (1993, 1999) and is quoted for the u filter data.

ID	Freq. (cd^{-1})	u Amp. (mmag)	v Amp. (mmag)	y Amp. (mmag)	S/N
f_1	5.86400 ± 0.00004	47.2	41.0	38.4	85.4
f_2	5.95059 ± 0.00007	35.0	20.6	17.3	63.4
f_3	6.18774 ± 0.00013	16.1	12.4	11.6	29.3
f_4	5.7094 ± 0.0005	4.0	3.2	3.6	7.1
$f_1 + f_2$	11.81459	1.7	1.7	1.7	3.2
$f_1 + f_3$	12.05174	2.3	1.8	1.7	4.3
$2f_2$	11.90118	2.2	1.6	1.8	4.1

3.3.1 Refining the determination of the pulsation frequencies

Although the photometry by Handler et al. (2003) was taken three years before the measurements presented in this paper, the frequency determinations of both works are accurate enough that we can link the previous V and the present y data to obtain more accurate pulsation frequencies. The effective wavelengths of these two bands are also sufficiently similar to render such an approach valid.

Consequently, we performed a joint frequency analysis with `Period 98`, where we could also reveal the presence of one more combination signal. The result is given in Table 4. We have confirmed that the frequencies of the three strongest modes and their combination frequencies are alias-free by including the HIPPARCOS photometry of the star (ESA 1997) as well. We could not make a similar check for mode f_4 due to its low amplitude. In any case, the residual amplitude spectrum after prewhitening our joint solution contains no evidence that measurable amplitude or frequency variations have occurred within the 3.4-y time base of our observations. We have also determined the Strömgren v amplitudes given this frequency solution for the combined 2002 and 2005 data. However, we could not do the same for the Johnson U and Strömgren u bands because their wavelength responses are sufficiently different that the calculated amplitudes of the strongest modes do not correspond within the errors.

4 MODE IDENTIFICATION

The spherical degree ℓ of the pulsation modes of our three target stars can be identified by comparing their observed *uvy* amplitudes with those predicted by theoretical models. Required input for these models are the mass and effective

Table 4. Multifrequency solution for the combined ground-based time-resolved V and y, as well as v photometry of KZ Mus. The error estimates (Montgomery & O'Donoghue 1999) on the amplitudes are ± 0.2 mmag. The S/N ratio was computed following Breger et al. (1993, 1999).

ID	Frequency (cd^{-1})	v Amp. (mmag)	V or y Amp. (mmag)	S/N
f_1	5.864016 ± 0.000005	41.2	38.4	109.5
f_2	5.950693 ± 0.000011	20.4	16.5	47.2
f_3	6.187472 ± 0.000016	12.3	10.9	31.4
f_4	5.70935 ± 0.00006	3.1	3.0	8.4
$f_1 + f_2$	11.814709	1.9	1.9	6.2
$2f_2$	11.901386	1.5	1.5	5.0
$f_1 + f_3$	12.051489	1.3	1.3	4.4
$f_2 + f_3$	12.138165	1.2	1.2	4.0

temperature of the stars, from which their luminosity obviously follows as well.

For KZ Mus, we simply adopt the values given by Handler et al. (2003), who derived $T_{\rm eff} = 26000 \pm 700$ K and $\log L/L_\odot = 4.22 \pm 0.20$. For the two stars in Canis Major, the calibrations by Crawford (1978) applied to the standard Strömgren photometry by Crawford, Barnes & Golson (1970) results in $E(b-y) = 0.027$ for β CMa and $E(b-y) = 0.031$ for 15 CMa, respectively. The Strömgren system calibration by Napiwotzki, Schönberner & Wenske (1993) then yields $T_{\rm eff} = 25600 \pm 1000$ K for β CMa and $T_{\rm eff} = 26300 \pm 1000$ K for 15 CMa.

With the Geneva colour indices of the two stars obtained from the Lausanne Photometric data base, the calibrations by Künzli et al. (1997) provide $T_{\rm eff} = 25100 \pm 1100$ K and $\log g = 3.3 \pm 0.6$ for β CMa, and $T_{\rm eff} = 26000 \pm 1500$ K and $\log g = 3.8 \pm 0.6$ for 15 CMa.

The analysis of IUE spectra of a number of β Cephei stars by Niemczura & Daszyńska-Daszkiewicz (2005) results in $T_{\rm eff} = 24700 \pm 800$ K and $\log g$=3.74 for β CMa and $T_{\rm eff} = 24600 \pm 1000$ K and $\log g$=3.81 for 15 CMa.

The HIPPARCOS parallax of β CMa is 6.53±0.66 mas. With V=1.98 and the reddening as determined before, we obtain $M_v = -4.1 \pm 0.2$. The parallax of 15 CMa (2.02±0.70 mas) is too inaccurate to be useful. However, 15 CMa is a member of the young open cluster Collinder 121, whose distance was determined as 592 ± 28 pc (de Zeeuw et al. 1999), which is in reasonable agreement with the usually quoted distance to the cluster in the pre-HIPPARCOS era, 630 pc (Feinstein 1967). Using the most recent distance to Collinder 121, we determine $M_v = -4.2 \pm 0.2$ for this star, given that V=4.80 and again adopting the amount of reddening suggested by Strömgren photometry.

Summarising the temperature determinations quoted before, we arrive at final values of $T_{\rm eff} = 25100 \pm 1200$ K for β CMa and 25600 ± 1200 K for 15 CMa. According to Flower (1996), these effective temperatures correspond to bolometric corrections of $BC = -2.2 \pm 0.3$ mag and $BC = -2.3 \pm 0.4$ mag, respectively. Consequently, the bolometric luminosities of the two stars are -6.3 ± 0.4 mag (β CMa) and -6.5 ± 0.4 mag (15 CMa), respectively.

Figure 8 shows the positions of our three targets in a theoretical HR diagram. The two stars in Canis Major have very similar properties there, indicating that both are massive and are approaching the end of their main sequence life.

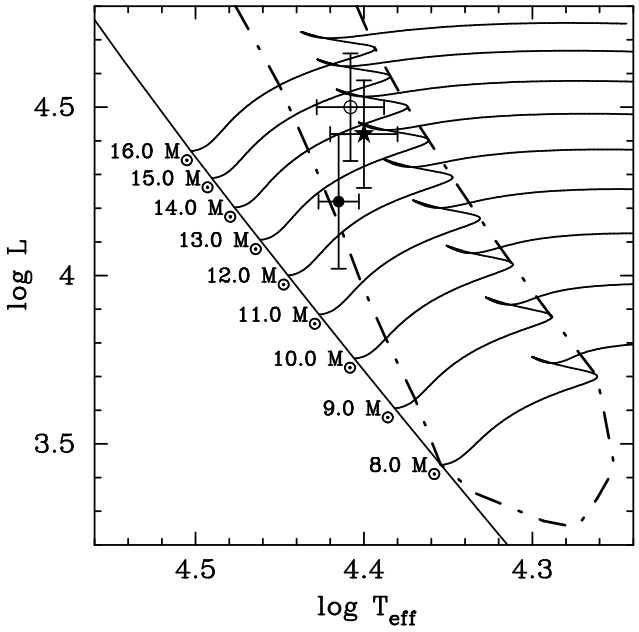

Figure 8. The positions of our three targets in the theoretical HR diagram. The filled circle denotes KZ Mus, the star symbol is for β CMa, and the open circle represents 15 CMa. Error estimates on the effective temperatures and luminosities of the stars are indicated. Some stellar evolutionary tracks, for a metal abundance of $Z = 0.02$, labelled with their masses (full lines) are included for comparison. We also show the theoretical borders of the β Cephei instability strip (Pamyatnykh 1999, dashed-dotted line).

This is somewhat in contrast with their distinctly different pulsation periods. KZ Mus appears to just have entered the instability strip and has lower mass than the two other pulsators.

For the purpose of mode identification we computed theoretical photometric uvy amplitudes for the $0 \leqslant \ell \leqslant 4$ modes of models with masses between 13.0 and 16.0 $M_\odot$ in steps of $1.0 M_\odot$, and in a temperature range of $4.38 \leqslant \log T_{\rm eff} \leqslant 4.43$ for β and 15 CMa. For KZ Mus, we investigated a range of 11.5 to 14.0 $M_\odot$ in steps of 0.5 $M_\odot$, and $4.395 \leqslant \log T_{\rm eff} \leqslant 4.435$, therefore applying a generous interpretation of the derived error bars. All models had an assumed metallicity of $Z = 0.02$. This approach is similar to that by Balona & Evers (1999).

Theoretical mode frequencies between 3.7 and 4.5 cd^{-1} were considered for β CMa, between 4.8 and 5.9 cd^{-1} for 15 CMa and between 5.4 and 6.5 cd^{-1} for KZ Mus. The frequency ranges chosen are somewhat larger than the ones excited in the stars to allow for some rotational m-mode splitting. We compare the theoretical photometric amplitude ratios to the observed ones in Figs. 9 to 11 for all independent modes of all three stars.

Starting with β CMa, it is clear that its strongest mode has a spherical degree of $\ell = 2$. The second mode seems radial, although its measured amplitude vs. wavelength dependence is considerably steeper than theoretically predicted. However, we believe that this is caused by problems with differential colour extinction, which artificially increases the measured u amplitude, as discussed in Sect. 3. In any case, no mode identification other than $\ell = 0$ is possible for this

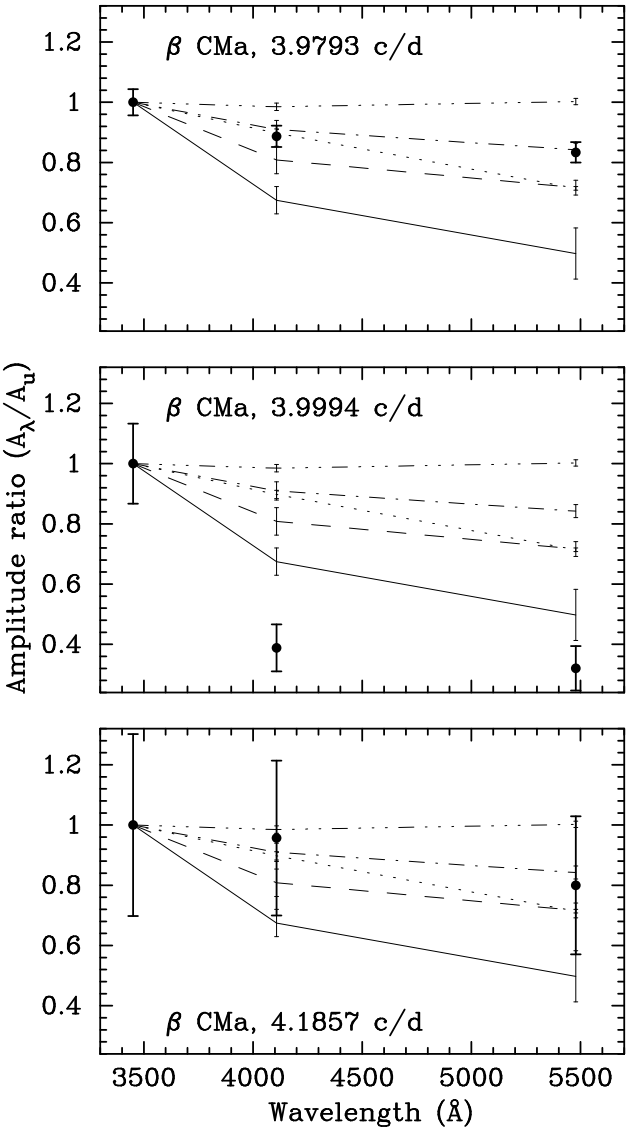

Figure 9. Mode identifications for β CMa from a comparison of observed and theoretical *uvy* amplitude ratios, normalised to unity at u. The filled circles with error bars are the observed amplitude ratios. The full lines are theoretical predictions for radial modes, the dashed lines for dipole modes, the dashed-dotted lines for quadrupole modes, the dotted lines for octupole ($\ell = 3$) modes, and the dashed-dot-dot-dotted lines are for $\ell = 4$. The thin error bars denote the uncertainties in the theoretical amplitude ratios.

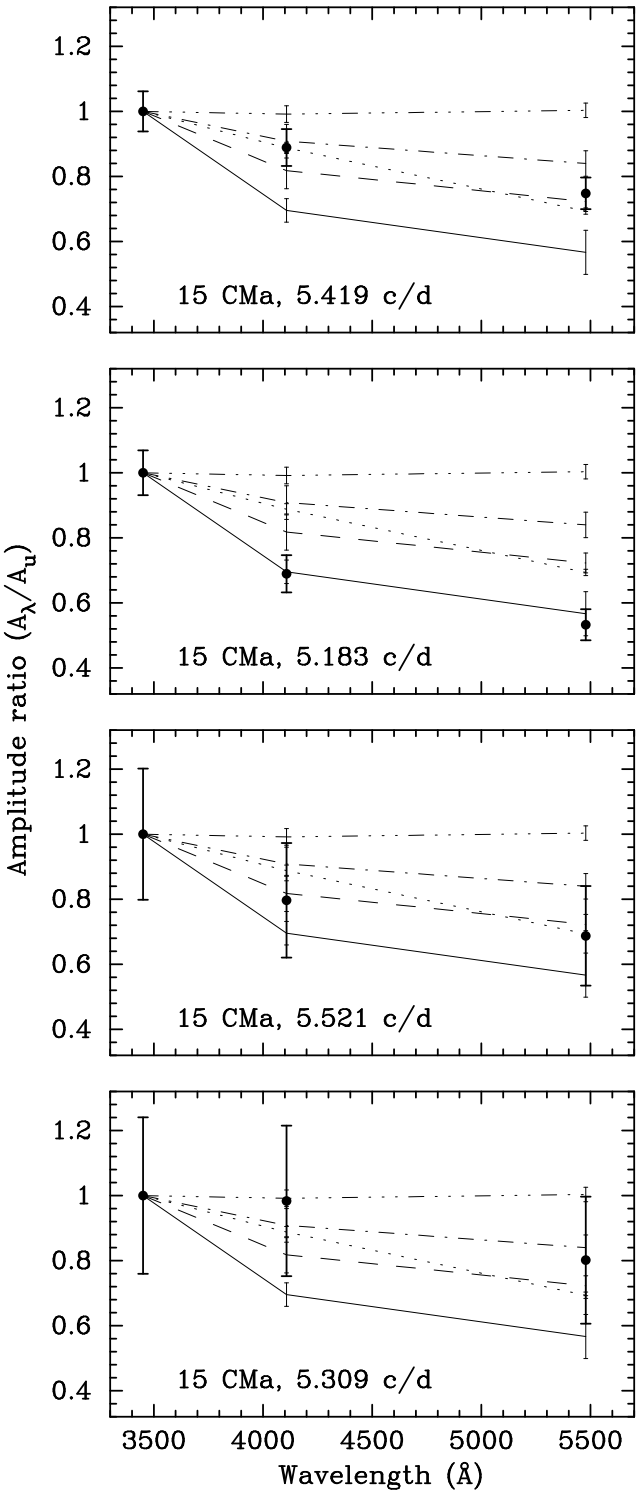

Figure 10. Mode identifications for 15 CMa from a comparison of observed and theoretical *uvy* amplitude ratios, normalised to unity at u. The filled circles with error bars are the observed amplitude ratios. The full lines are theoretical predictions for radial modes, the dashed lines for dipole modes, the dashed-dotted lines for quadrupole modes, the dotted lines for $\ell = 3$ modes, and the dashed-dot-dot-dotted lines are for $\ell = 4$. The thin error bars denote the uncertainties in the theoretical amplitude ratios.

mode. The lowest-amplitude pulsation mode is nonradial, but its spherical degree cannot be constrained due to its small amplitude.

Continuing with 15 CMa, we see that the strongest mode is nonradial with $\ell = 1$, 2 or 3, but no distinction between these hypotheses can be made. The second strongest mode is most likely radial, and no mode identification is possible for the two weakest modes. However, due to their proximity to the radial mode in frequency, they must be nonradial.

Turning to KZ Mus, one immediately sees that its strongest mode is $\ell = 2$. The second strongest mode is sug-

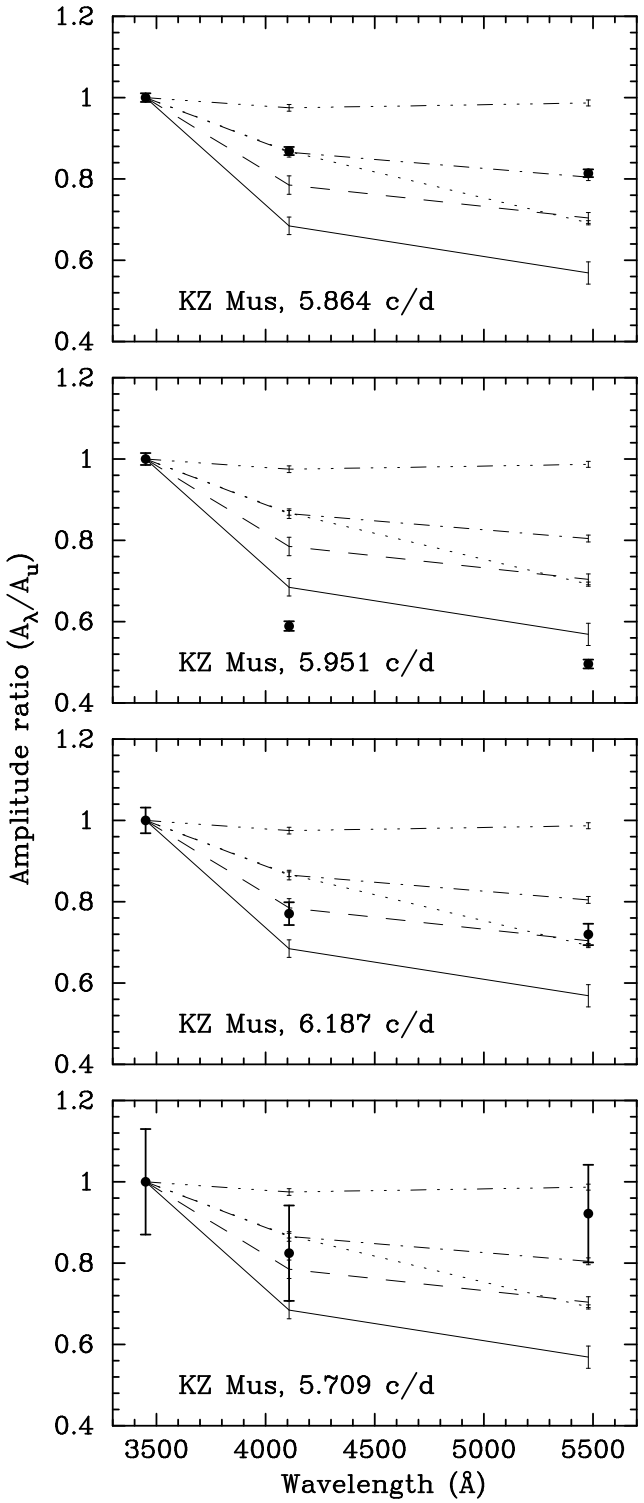

Figure 11. Mode identifications for KZ Mus from a comparison of observed and theoretical *uvy* amplitude ratios, normalised to unity at *u*. The filled circles with error bars are the observed amplitude ratios. The full lines are theoretical predictions for radial modes, the dashed lines for dipole modes, the dashed-dotted lines for quadrupole modes, the dotted lines for octupole modes, and the dashed-dot-dot-dotted lines are for $\ell = 4$. The thin error bars denote the uncertainties in the theoretical amplitude ratios.

gested to be radial, although again the observed amplitude ratios indicate a steeper wavelength dependence of the amplitudes than theoretically predicted. The third mode of KZ Mus is a dipole, $\ell = 1$, and the fourth is nonradial. These results are in perfect agreement with the mode identifications by Handler et al. (2003).

5 DISCUSSION AND CONCLUSIONS

We have observed the three β Cephei stars because we aimed at new and improved mode identifications and because we wanted to check whether these objects would justify a larger observational effort for asteroseismic purposes. We have reasonably succeeded in providing the mode identifications.

One point that appears problematic, however, is that the theoretically predicted u/v and u/y amplitude ratios for radial modes are smaller than the measured ones for β CMa and KZ Mus. Whereas the reason for this discrepancy may be incorrect differential colour extinction coefficients for β CMa that directly affect the measured amplitudes of the $3.9994\mathrm{cd}^{-1}$ mode, we cannot invoke this explanation for the $5.951\mathrm{cd}^{-1}$ mode of KZ Mus as its frequency is too different from an integer multiple of one cycle per sidereal day. In addition, the theoretical and observed $UvBV$ amplitudes derived by Handler et al. (2003) are in perfect agreement for a radial mode in this star. We note that we have used the same differential colour extinction correction for β and 15 CMa, which was derived from the 15 CMa data only. These two stars were measured simultaneously, and have very similar colours, which is why this procedure was soundest.

Returning to the mode identifications of the individual stars, the two strongest modes of β CMa are a quadrupole and likely a radial mode. Given the effective temperature, luminosity and thus mass inferred in Sect. 4, we can compute the pulsation "constant" for such a radial mode. The result of this calculation is $Q = 0.035 \pm 0.009$ d, indicating that this mode may be the radial fundamental, although the possibility that it is the first overtone cannot be ruled out this way.

We were also able to locate a radial mode in the pulsation spectrum of 15 CMa, whose pulsation constant would be $Q = 0.027 \pm 0.007$ d. This suggests that we deal with the first radial overtone in this case, although the fundamental mode or the second overtone can also not be excluded. We note, however, that no convincing detection of a radial mode in a β Cephei star other than the fundamental has been made to date.

Three of the nonradial pulsation modes of 15 CMa are almost equally spaced in frequency. Regrettably, we cannot be sure whether these modes are $\ell = 1$, 2 or 3. Independent of the ℓ value, we can still assume that these modes do correspond to rotationally split components of the same mode to check whether this leads to reasonable results.

Doing so, and further assuming that the observed splitting corresponds to the surface rotational frequency of 15 CMa, we derive a rotation period of 9.35 d, which translates into an equatorial rotational velocity of $49 \pm 8\,\mathrm{kms}^{-1}$. The measured $v \sin i$ of 15 CMa is $40\,\mathrm{kms}^{-1}$ (Uesugi & Fukuda 1982), making it possible that the three nonradial modes of the star indeed belong to the same k and ℓ.

For KZ Mus we confirmed the mode identifications by

Handler et al. (2003). Unfortunately, the ℓ value of the weakest known independent mode of the star can still not be uniquely constrained. Repeated observations in the future may help to solve this problem as measurements from different years can be analysed together, if homogeneous filter sets (particularly bluewards of the Balmer jump) are used. If a mode identification of f_4 can be derived, we believe it is likely that theoretical asteroseismic investigations can be undertaken. Of course, additional measurements in the future may also help to reveal modes beyond our present detection limit (1.5 mmag).

To our regret, the asteroseismic prospects of β CMa do not seem to be very high. With only three modes photometrically detected and only two identified with their ℓ value, a detailed exploration of its inner structure seems unlikely. Perhaps this bright star is better studied by means of spectroscopy, for instance as done by Briquet et al. (2006).

15 CMa seems more worthwhile for further study. We have proven the existence of a radial mode, which is of tremendous importance for restricting the star's location in the HR diagram. We have also found evidence that the remaining three nonradial modes may form a rotationally split triplet, which can be the starting point for an asteroseismic study. What still needs to be done is to prove that this is indeed a mode triplet and to determine its ℓ value.

An independent clue towards the spherical degree of this possible triplet may come from its frequency asymmetry due to the second-order effect of rotation, which is different for different ℓ. Following the definition of the asymmetry of a frequency triplet $f_- < f_0 < f_+$ by Dziembowski & Jerzykiewicz (2003):

$$A_{obs} = f_- + f_+ - 2f_0,$$

we obtain $A = -0.0077 \pm 0.0015 \mathrm{cd}^{-1}$ from our measurements and $A = -0.0004 \pm 0.0011 \mathrm{cd}^{-1}$ from the archival data. These two values are inconsistent (perhaps due to systematic frequency errors in the single-site archival data) and can therefore not be interpreted; more time-resolved measurements are needed.

An unusual feature in the light curves of 15 CMa is that the descending branch of the strongest mode's pulsation is steeper than its rising branch. In fact, even a "stillstand" phenomenon is indicated. This has been found in only one β Cephei star, BW Vul, to date (e.g. see Sterken et al. 1986) and is usually interpreted as a shock phenomenon in the atmosphere due to the vicious acceleration of the stellar material due to pulsation (e.g. Fokin et al. 2004).

However, there are two differences between the pulsations of BW Vul and 15 CMa: BW Vul pulsates in a single radial mode, and with much higher photometric amplitude than 15 CMa, whose mode showing the unusual light curve form is nonradial. The small photometric amplitude can be explained under the assumption that the strongest mode of 15 CMa is the $m = 0$ component of a rotationally split multiplet. The possible range in the inclination of the pulsation axis to the line of sight may lead to heavy geometrical cancellation of such a mode (e.g. see Pesnell 1985). In other words, this mode could have high intrinsic amplitude and its low photometric amplitude is just a projection effect.

The unusual light curve form of this mode naturally gives rise to a harmonic frequency with high relative amplitude compared to the mode causing it. Combination frequencies with abnormally high amplitudes could in some cases also be caused by resonant mode coupling (see Handler et al. 2006 for a more detailed discussion), whereas other combination frequencies may be simple light-curve distortions caused by a nonlinear response of the flux to a sinusoidal displacement due to pulsation. The sum frequencies we found in the amplitude spectra of KZ Mus seem to be such "normal" combinations. Their relative amplitudes are in the same range as those of the "normal" combinations of the β Cephei stars 12 Lac (Handler et al. 2006) and ν Eri (Handler et al. 2004, Jerzykiewicz et al. 2005), keeping in mind inclinational effects. Resonant mode coupling is therefore not required to explain the combination frequencies of KZ Mus.

Finally, we noticed the occurrence of slow intrinsic variability in our residual light curves for β and 15 CMa. Such variations have been reported for several other β Cephei stars (see the discussion by Handler et al. 2006), and seem to be a fairly common phenomenon. Despite the existence of very extensive data sets, its physical cause remains unknown.

ACKNOWLEDGEMENTS

This work has been supported by the Austrian Fonds zur Förderung der wissenschaftlichen Forschung under grants R12-N02 and P18339-N08.

This paper has been typeset from a TEX/ LATEX file prepared by the author.

REFERENCES

Balona L. A., Evers E. A., 1999, MNRAS 302, 349
Balona L. A., Bregman L., Letsapa B. A., Magoro B. T., Walsh S. E., 1996, IBVS 4313
Breger M., et al., 1993, A&A 271, 482
Breger M., et al., 1999, A&A 349, 225
Briquet M., et al., 2006, A&A, submitted
Campbell, W. W., 1911, Lick. Obs. Bull. 6, 140
Crawford D. L., 1978, AJ 83, 48
Crawford D. L., Barnes J. V., Golson J. C., 1970, AJ 75, 624
Dziembowski W. A., Jerzykiewicz M., 2003, in *International Conference on magnetic fields in O, B and A stars*, ed. L. A. Balona, H. F. Henrichs & R. Medupe, ASP Conf. Ser. Vol 305, p. 319
ESA, 1997, The *Hipparcos* and *Tycho* catalogues, ESA SP-1200
Feinstein A., 1967, ApJ 149, 107
Fokin A., Mathias P., Chapellier E., Gillet D., Nardetto N., 2004, A&A 426, 687
Handler G., 2005, IBVS 5667
Handler G., et al., 2000, MNRAS 318, 511
Handler G., Shobbrook R. R., Vuthela F. F., Balona L. A., Rodler F., Tshenye T., 2003, MNRAS 341, 1005
Handler G., et al., 2004, MNRAS 347, 454
Handler G., et al., 2006, MNRAS 365, 327
Heynderickx D., 1992, A&AS 96, 207
Heynderickx D., Waelkens C., Smeyers P., 1994, A&AS 105, 447
Jerzykiewicz M., Handler G., Shobbrook R. R., Pigulski A., Medupe R., Mokgwetsi T., Tlhagwane P., Rodríguez E. 2005, MNRAS 360, 619
Kołaczkowski Z., et al. 2004, ASP Conf. Ser. 310, 225

Künzli M., North P., Kurucz R. L., Nicolet B., 1997, A&AS 122, 51
Montgomery M. H., O'Donoghue D., 1999, Delta Scuti Star Newsletter 13, 28 (University of Vienna)
Moore J. H., 1936, Lick. Obs. Bull. 18, 1
Niemczura E., Daszyńska-Daszkiewicz J., 2005, A&A 433, 659
Pamyatnykh A. A., 1999, Acta Astr. 49, 119
Pamyatnykh A. A., Handler G., Dziembowski W. A., 2004, MNRAS 350, 1022
Pesnell W. D., 1985, ApJ 292, 238
Pigulski A., 2005, Acta Astr. 55, 219
Shobbrook R. R., 1973a, MNRAS 161, 257
Shobbrook R. R., 1973b, MNRAS 162, 25
Stankov A., Handler G., 2005, ApJS 158, 193
Sterken C., et al., 1986, A&AS 66, 11
Struve O., 1950, ApJ 112, 520
Uesugi A., Fukuda I., 1982, *Catalogue of stellar rotational velocities (revised)*, University of Kyoto
de Zeeuw P. T., Hoogerwerf R., de Bruijne J. H. J., Brown A. G. A., Blaauw A., 1999, AJ 117, 354